Frequency Optimization for Narrowband Power-Line Communications

T. O. Sanya, T. G. Swart, and H. C. Ferreira

Dept. of Electrical and Electronic Engineering Science,
University of Johannesburg,
P.O. Box 524, Auckland Park, 2006, South Africa,
Email: {tosanya, tgswart, hcferreira}@uj.ac.za

***Abstract*—Optimized frequency tones for the power line channel is presented from an experimental scenario. Four sets of frequency tones, grouped according to CENELEC's regulation on frequency use for narrow band power line applications are selected according to their signal-to-noise ratio (SNR) performance. COMBLOCKS, a prototyping hardware was used for the implementation. Often times, M-FSK/OFDM have been presented and used as the modulation scheme of choice for power line communications (PLC), the choice of best frequencies to use is however, an area that has hardly been explored. This paper is concentrated on the choice of such optimal frequencies.**

***Index Terms*—MFSK, OFDM, Comblocks, Power Line Communications, Signal-to-noise ratio, Attenuation, Noise.**

I. Introduction

The commercial use of PLC has lacked a significant commercial take-off for decades, with reliability being the major problem. This paper presents measurements made from the implementation of M-FSK as a modulation scheme for transmission of information over the power line. This scheme has been highlighted in many literatures to be robust against noises such as; the additive white Gaussian noise, background noise and the most severe impulse noise, which adversely affects signal quality over the power line channel [1]–[3]. The robust attribute of this scheme has made it the modulation scheme of possible choice for PLC applications. However, hardly anything has been found in literature where the use of frequencies has been investigated for optimised performance on PLC. This work is also motivated by the work done by Ferreira *et al*. [1], where permutation trellis codes combined with M-FSK, were proposed to be robust against noises over power line, impulse noise especially. This work therefore creates the ground work to implementing what was proposed in [1]. Also, with the advent of PLC G3 and Prime, [11], this work serves as a ground work for their implementation.

II. M-FSK Modulation Scheme of Choice

This modulation scheme has the advantages of constant envelope modulation, detection can be done coherently and non-coherently, it is relatively easy to construct, frequency diversity, and the probability of error becomes lower as M increases, provided the SNR does not exceed the Shannon limit of -1.6 dB [3]. In [3] the expression for an M-FSK signal is given as:

$$S_i(t) = \sqrt{2E_s/T_s}\cos(2\pi f_i t); \quad 0 \le t \le Ts, \tag{1}$$

where $i = 1, 2, \ldots, M$ and E_s is the signal energy per modulated symbol,

$$f_i = f_0 + (i+1)/T_s; \quad 1 \le i \le M. \tag{2}$$

The major short fall of this scheme is that it is not spectrally efficient. As the M-ary number increases, the spectral efficiency reduces. Also, a major trade-off in this scheme is the higher cost of bandwidth. M-FSK requires more bandwidth which also increases as the M-ary number increases [3]. The bandwidth efficiency is given by the relation:

$$\rho = \log_2 M/M. \tag{3}$$

In [4], it was summarily stated that phase shift keying (PSK) is more appropriate in a system where phase coherent detection can be achieved while FSK is preferable in a system where phase coherent transmission cannot be guaranteed. M-FSK has also been compared with other spread spectrum techniques for PLC applications. While OFDM outperforms CDMA both in the narrowband and broadband PLC [5], [6], M-FSK's performance was found to be better than that of CDMA in terms of their bit error rate performance [7].

III. Coupling Circuitry

Figs. 1 and 2 show the circuit diagram of the coupling circuits. R_s and R_p are the impedance values of the power line. Grounding the center point of the zener diodes incorporates common mode protection. The effect of this has been investigated and presented in [8]. The bandwidth of these coupling circuits can be determined by calculating their -3dB low and high frequency values. The 'TX' has a bandwidth calculated as 7.96 kHz – 1.19 MHz, while the 'RX' is calculated to the values of 7.96 kHz – 11.366 MHz. The circuit parameters are all referred to the power line side.

Fig. 3 shows the frequency response of the coupling circuitry used for this experiment. It can be observed that the 'TX' (used on the transmit side) voltage value increases with increasing frequency until a high frequency value of 7.5 kHz, considering the -3dB cut-off [9]. The response has a pass band up until 1 MHz. We consider this as a good response

as it covers the useful spectrum of the CENELEC band. The circuitry is essential for protection of communication equipment both at transmit and receive side by filtering the 50 Hz power signal.

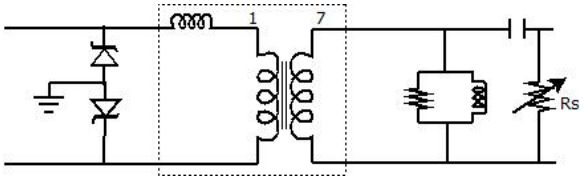

Fig. 1. Coupling circuit "TX".

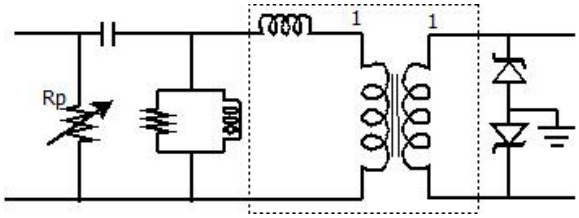

Fig. 2. Coupling circuit "RX".

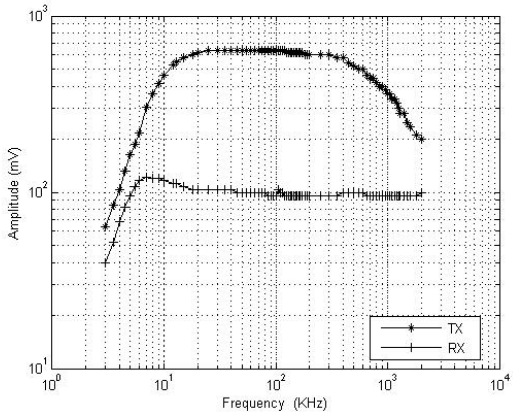

Fig. 3. Coupling circuit response.

The resonant frequencies of both circuits are calculated using the relations:

$$f_R = 1/(2\pi\sqrt{LC}), \tag{4}$$

where L and C are the respective leakage inductance and series capacitance values. The 'TX' was calculated to resonate at 232.1 kHz while the 'RX' calculated resonance value is 90 kHz.

IV. Implementation

This section presents the various stages of the implementation as well as the characteristics of each of the prototyping equipment used (hereon after called Comblocks). Fig. 4 is a picture of the complete implementation setup. It comprises of a TCP/IP interface card, arbitrary waveform generator, M-FSK modulator, digital to analog converter. Each of these units has their properties, for comprehensive details, the reader is referred to [6]. Here, the Comblocks modules are briefly described:

- TCP/IP interface card (Com5003): it interfaces between the Comblocks assembly and the user. It facilitates the upload/download of data (which has been stored on the PC in a suitable file format) to/from Comblocks assembly.
- M-FSK digital Modulator (Com1028): This module contains a numerically controlled oscillator (NCO), which generates pseudo random number sequence, and modulates them according to the M-ary settings. It has settings for 2-, 4-, and 8-ary M-FSK. This module operates in both broadband and narrowband spectrum, but it is optimised for broadband use. This module outputs a continuous phase frequency shift keying (CPFSK) signal. The carrier frequency is modulated based on the PN sequence and the modulation index settings.
- D/A Converter (Com2001): Communication is in digital form up to this stage in the Comblocks assembly. This module therefore converts the digital modulated signal into analog form for transmission over the power line.

Both Com1028 and Com2001 have a very low power output (Fig. 5). Their combined frequency response curve is presented in Fig. 6 with the coupling circuits connected back-to-back. The region marked "A" is the CENELEC's allowed band for narrowband PLC. An L165 operational amplifier is used to boost the power of the signal. Fig. 7 shows the setup of the buffer circuits, while Fig. 8 is the response after the signal has been boosted. The buffer circuit's non-uniform output should be noted, considering the fact that a unity gain amplifier was used. This is as a result of the transmit side coupling circuit, which is a step-up transformer.

Using the op-amp implies adding more noise to the channel, but it is a good trade-off as long as the SNR is at an acceptable level for signal detection.

The narrowband (0–200 kHz) characteristic of the L165 op-amp is responsible for the sharp drop after 200 kHz in the response curve of Fig. 8. Since the bandwidth for narrowband PLC applications according to CENELEC is between 3–148.5 kHz, this op-amp is suitable for the purpose of this work.

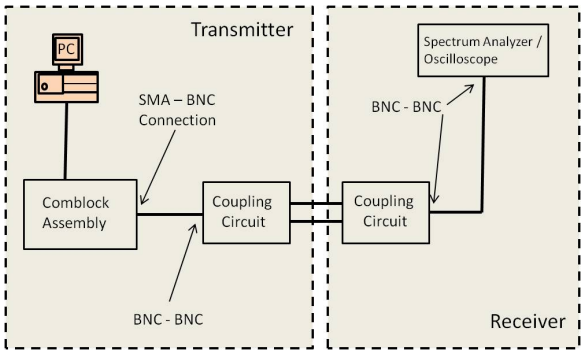

Fig. 4. Implementation setup.

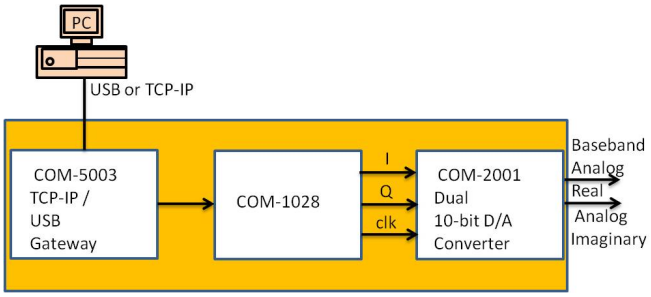

Fig. 5. Comblock assembly.

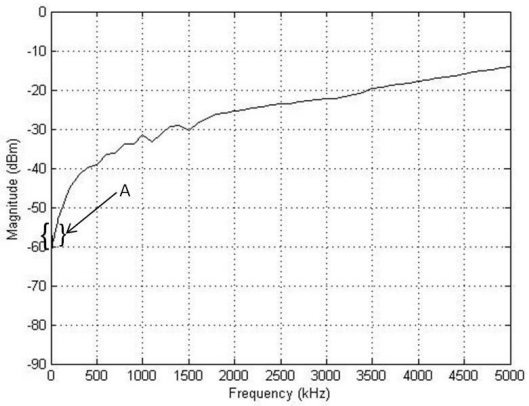

Fig. 6. Comblock's low output signal power.

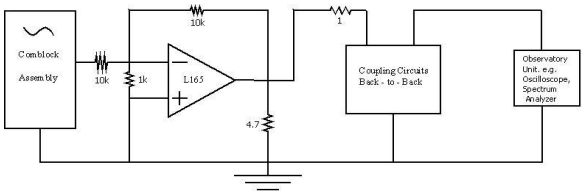

Fig. 7. Buffer circuit for Comblocks' output signal.

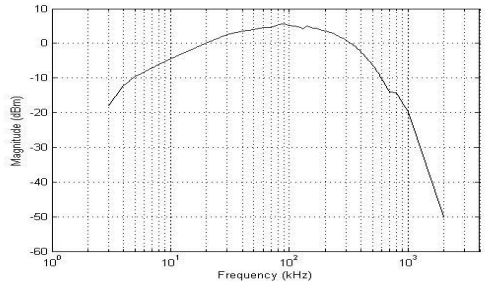

Fig. 8. Buffer circuit output power.

V. Stepwise Procedure in Choosing Optimal Frequencies

The CENELEC's band for narrowband PLC is divided into four classes. We however group these bands into three groups as listed below:

1) Group A: 3 – 95 kHz
2) Group B: 95 – 125 kHz
3) Group C: 125 – 148.5 kHz

Classes C and D in the CENELEC band were combined together because of their very narrow band, also, their area of application are closely related.

The University laboratory was used as the test environment. This environment is characterized by desktop computers with switch mode power supplies, CRT and flat screen monitors, printers, fluorescent lamps, and air conditioners. The signal quality was first tested by connecting the coupling circuits back-to-back without the power line. An HP 8591E spectrum analyzer was used for measurement. We started the implementation by first testing the versatility of the prototyping equipment. This is done by connecting the transmitter and receiver back-to-back. The power line is then introduced with the back-to-back connection. Comparing Fig. 9 and Fig. 10, the effect of the power line on the signal is evident where a signal loss of 15 dBm is recorded in the middle of the spectrum. A worst case scenario of 30 dBm signal loss is also recorded around 140–150 kHz. The prominent noise around 50–70 kHz should also be noted, this spectrum has very low SNR, and it therefore should be avoided for any use. This procedure was repeated for distances 3 m, 5 m, and 10 m respectively. The results are presented in Figs. 11–13. The low SNR observed at the higher frequency with the 10 m can be improved by increasing the signal power or having a repeater on the channel.

In all the instances of our measurements, the received signal power as well as the noise signal power was recorded in a spreadsheet, their SNR values were calculated according to [10]:

$$\text{SNR} = (S/N)_b, \tag{5}$$

where S is the received signal power and N the noise power.

The SNR results were processed by sorting the best values in all the distance instances with respect to their different groups. These best frequencies were then plotted on a bar graph. The frequencies with the highest number of occurrence in the different distances emerge as the best. These results are further shown in Figs. 14–16. The combined SNR performance of all the frequencies at different distance of measurement is further shown in Fig. 17.

VI. Discussion

Evident from Figs. 14–16, the best frequency tones are listed below:

- Group A: 75 kHz, 80 kHz, 85 kHz, 90 kHz.
- Group B: 95 kHz, 100 kHz, 105 kHz, 112 kHz.
- Group C: 125 kHz, 130 kHz, 132 kHz, 135 kHz, 148 kHz.

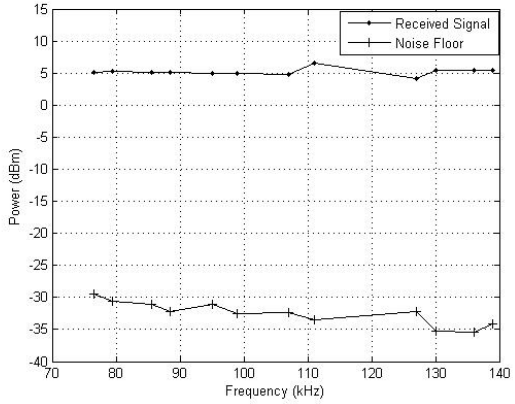

Fig. 9. Back-to-back connection without power line.

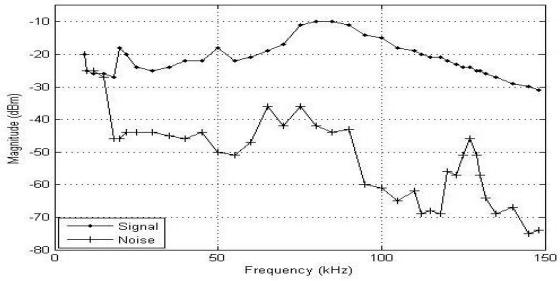

Fig. 10. Back-to-back connection with power line.

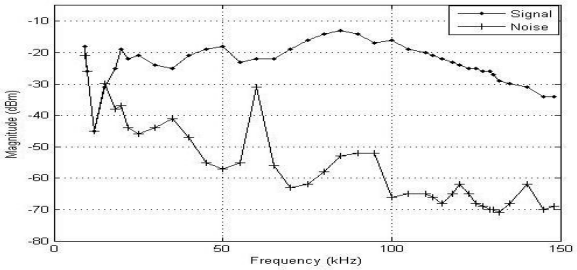

Fig. 11. SNR at 3 m.

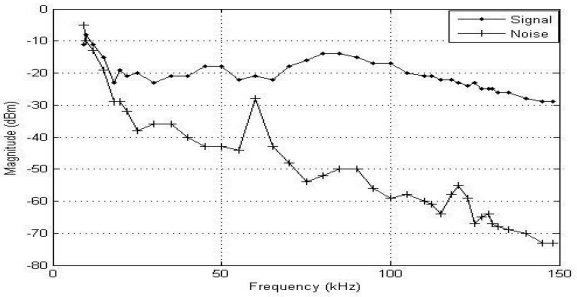

Fig. 12. SNR at 5 m.

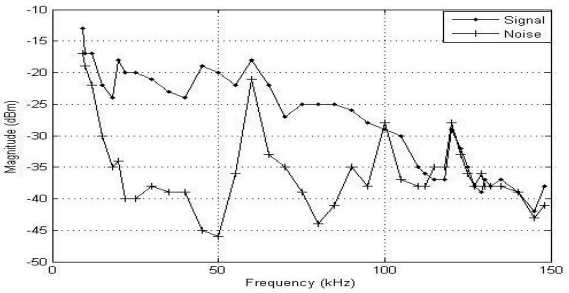

Fig. 13. SNR at 10 m.

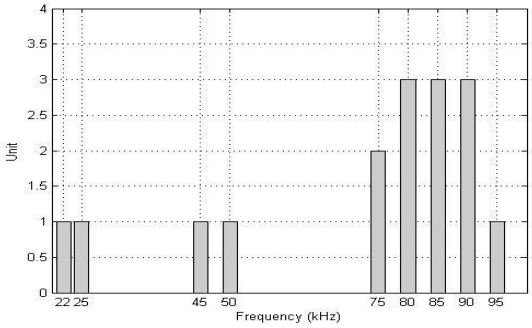

Fig. 14. Best frequency selection for Group A.

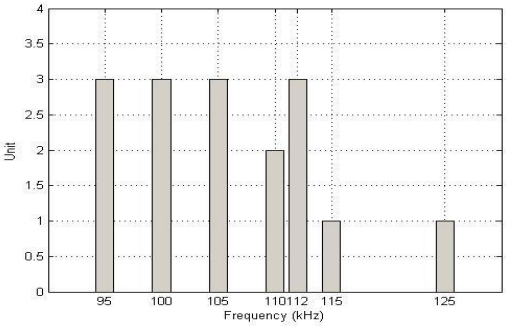

Fig. 15. Best frequency selection for Group B.

Comblocks was used to implement M-FSK on the power line channel. Since the Comblocks M-FSK signal generator is a continuous phase frequency shift keying (CPFSK) signal generator, the following frequencies were implemented after configuring the hardware:

- Group A: 76.5 kHz, 79.5 kHz, 85.5 kHz, 88.5 kHz.
- Group B: 95 kHz, 99 kHz, 107 kHz, 111 kHz.
- Group C: 127 kHz, 130 kHz, 136 kHz, 139 kHz.

These groups of frequency were further tested over the power line at different distances 3 m, 5 m, and 10 m, and back-to-back respectively, their received signal power compared with the noise power is shown in Figs. 18–21.

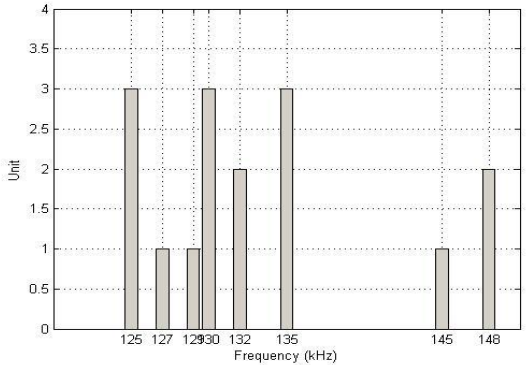

Fig. 16. Best frequency selection for Group C.

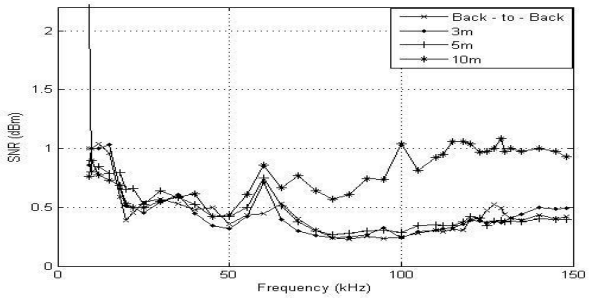

Fig. 17. SNR at different distances.

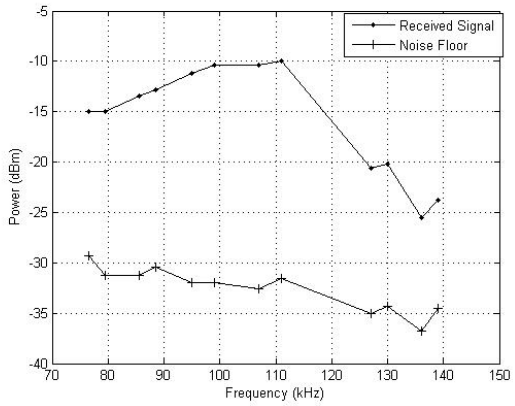

Fig. 18. Best frequencies (back-to-back).

The following deductions were also made from the experiment:

- The signal attenuates as the transmitter-receiver distance increases.
- The SNR is also influenced by the type of load connected between the transmitter and the receiver.
- A noise of relative high magnitude is constantly measured at approximately 61 kHz (Fig. 17). The noise power however varies at different instance of measurements.
- More noise was introduced into the channel as a result of the booster circuit used for this work.
- The power line is so dynamic that different signal power at a given frequency can be measured at different times.

It can also be seen from Fig. 18 that the impedance of the power line channel contributes significantly to loss of signal. This is found to be a function of distance between

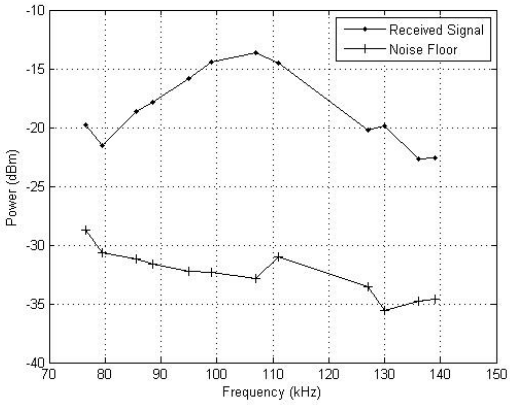

Fig. 19. Best frequencies (3 m).

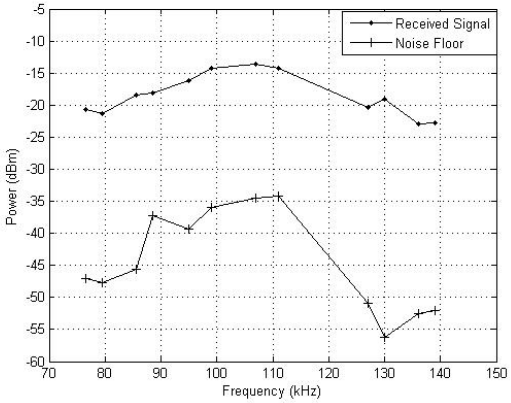

Fig. 20. Best frequencies (5 m).

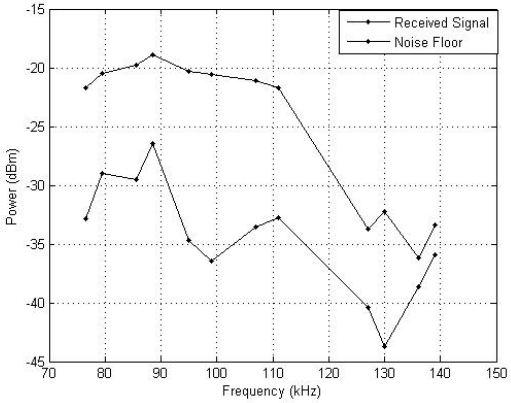

Fig. 21. Best frequencies (10 m).

the transmitter-receiver pairs.

VII. Conclusion

In this paper, Comblocks have been used to demonstrate frequency optimization over the power line. The dynamic nature of the power line is established with variance in the measurement parameters with respect to time. Although the result is not presented in this paper, a residential building was also used to confirm our results from the lab. It was observed that the noise environment was different. This implies that an extensive search is required to determine the best frequencies appropriate for different noise environments. Therefore, the choice of frequency or modem for optimal use will depend on the noise environment involved. Another possible solution would be to design an adaptive modem for the different noise environments.

Finally, it must be noted that this is an experiment carried out in a University laboratory in South Africa. A similar exercise is going on in Germany, for comparison between the different power line environments.

References

[1] H. C. Ferreira, A. J. H. Vinck, T. G. Swart, and I. De Beer, "Permutation trellis codes," *IEEE Trans. Commun.*, vol. 53, no. 11, pp. 1782–1789, Nov 2005.

[2] K. M. Dostert, "Telecommunication over the power distribution grid: Possibilities and limitations," in *Proc. Int. Symp. Power Line Commun. and its Appl.*, Essen, Germany, Apr. 2–4, 1997, pp. 1–9.

[3] A. J. H. Vinck, "Coded modulation for power line communications," in *Proc. A.E.U. Int. J. Elec. Commun.*, vol. 54, no. 1, Nov. 2000, pp. 45–49.

[4] L. A. Glover and P. M. Grant, *Digital Communications*, 2nd Ed., Pearson Prentice Hall, 2004.

[5] Y. H. Ma, P. L. So and E. Gunawan, "Comparison of CDMA and OFDM systems for broadband power line communications," *IEEE Trans. Power Delivery*, vol. 23, no. 4, pp. 1876–1885, Oct. 2008.

[6] E. Del Re, R. Fantacci, S. Morosi, and R. Seravalle, "Comparison of CDMA and OFDM techniques for downstream power-line communications on low voltage grid," *IEEE Trans. Power Delivery*, vol. 18, no. 4, pp. 1104–1109, Oct. 2003.

[7] A. Chandra and R. Hazarika, "A comparative study of MFSK and CDMA for power line communication with background Nakagami noise," in *Proc. IEEE Symp. Industrial Elec. and Appl.*, Penang, Malaysia, Oct. 3–5, 2010, pp. 195–200.

[8] T. O. Sanya, M. Hove, A. J. Snyders, and H. C. Ferreira, "Surge protection of communication equipment for power line communications: Effects on communication signal," in *Proc. IEEE Region 8 AFRICON*, Livingstone, Zambia, Sep. 13–15, 2011.

[9] P. A. Janse van Rensburg and H. C. Ferreira, "Coupling circuitry: Understanding the functions of different components," in *Proc. Int. Symp. Power Line Commun. and its Appl.*, Kyoto, Japan, Mar. 26–28, 2003, pp. 204–209.

[10] J. G. Proakis and M. Salehi, *Communication Systems Engineering*, Prentice Hall, 1st Ed., 1994.

[11] Martin Hoch, "Comparison of PLC G3 and Prime," in *Proc. Int. Symp. Power Line Commun. and its Appl.*, Udine, Italy, Apr. 3–6, 2011, pp. 165–169.